Synthetic Methods

Special Collection

One-Pot Dual C–C Coupling Reaction via Site Selective Cascade Formation by Pd^{II}-Cryptate of an Amino-Ether Heteroditopic Macrobicycle

Sayan Sarkar, Piyali Sarkar, Sandip Munshi, and Pradyut Ghosh*[a]

Abstract: Selectivity of aryl iodo over ethynyl iodo toward the Suzuki cross coupling reaction is explored by utilizing a palladium complex of amino-ether heteroditopic macrobicycle. Subsequently, unreacted ethynyl iodide undergoes homocoupling reaction in the same catalytic atmosphere, thereby representing a cascade dual C–C coupling reaction. Furthermore, this approach is extended for novel one-pot synthesis of unsymmetrical 1,3-diynes.

Introduction

The Suzuki coupling reaction is recognized to be one of the most effective reactions for the construction of a carbon-carbon bond between organoboron and organic halides.[1] Recently, the scope of this coupling reaction has been extended its path from $C(sp^2)$–$C(sp^2)$ bond formation to $C(sp^2)$–$C(sp^3)$ bond,[2] $C(sp^3)$–$C(sp^3)$ bond[3] and $C(sp^2)$–C(sp) bond[4] formation reactions, but selective Suzuki coupling among various $C(sp/sp^2/sp^3)$–X groups is itself a challenging task. Moreover, homocoupling reaction of C(sp)–X (X = halogens) substrates[5] can be in competition with its Suzuki coupling,[6] as both require nearly same catalytic conditions (Scheme 1 a). On the other hand, 1,3-diynes are important building blocks in material science[7] and organic synthesis[8] due to their unique linear structure and profuse reactivity. These diynes exemplifies as the important skeleton for the synthesis of natural products,[9] supramolecular architectures,[10] organic conductors,[11] electron-rich materials,[12] and so on. Among various synthetic techniques, alkynyl halide substrates may couple to form 1,3-diynes in certain reaction medium with considerable yields.[13] However, formation of biaryl substituted 1,3-diynes from alkynyl halides in presence of organoborons has not been investigated, as both homocoupling and Suzuki coupling of alkynyl halide might occur in a competitive manner, thus, it is hard to control the synthesis of regioselective product.[14] Single substrate having both aryl iodo and alkynyl iodo groups in Suzuki coupling conditions generally produces scramble of products due to the possibility of different types of reactions. Selective protection of a particular group may effectively channelize the reaction pathway in such a way that not only the Suzuki coupling occurs at the aryl iodo centre, but also homocoupling predominates at alkynyl iodo centre to produce the desired product selectively.

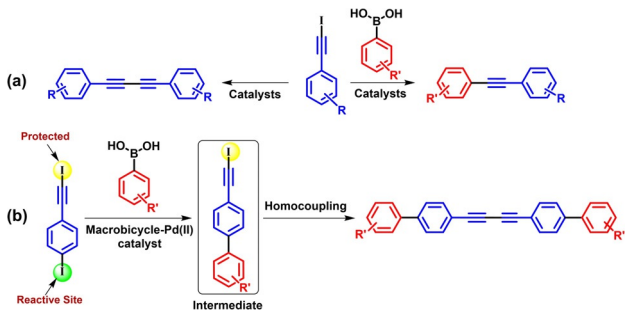

Scheme 1. (a) Different competitive C–C coupling reactions. (b) This report.

Herein, we have studied one-pot dual coupling of ethynyl iodo based aryl iodo substrates through site selective Suzuki coupling of aryl iodo center without hampering ethynyl iodo group, followed by consecutive homocoupling of C(sp) atoms (Scheme 1 b). This site selectivity has been achieved upon exploring an oxyether-amine based heteroditopic macrobicycle,[15] **L1** (Figure 1) as an additive in Pd^{II} catalytic environment. To the best of our knowledge, driving a substrate for a one-pot transformation through selective Suzuki coupling on

[a] S. Sarkar, Dr. P. Sarkar, S. Munshi, Prof. P. Ghosh
School of Chemical Sciences
Indian Association for the Cultivation of Science (IACS)
2A and 2B Raja S.C. Mullick Road, Jadavpur, Kolkata 700032, West Bengal (India)
E-mail: icpg@iacs.res.in

Supporting information and the ORCID identification number(s) for the author(s) of this article can be found under: https://doi.org/10.1002/chem.202005397.

This manuscript is part of an Indo-German special collection.

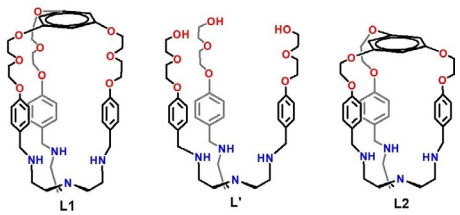

Figure 1. Chemical representations of **L1**, **L'** and **L2**.

C(sp^2)–X group without attacking C(sp)–X group by organoborons and successive homo coupling of C(sp) atom has not been investigated till date.

Results and Discussion

Selection of macrobicyclic cage and substrates

It is worth mentioning that a 3D cage moiety having well-defined functional groups can frame a guest with efficient binding capability.[16] On the other hand, different functionalities may provide site selective protective binding towards a specific group in presence of different labile groups of a guest molecule.[17] The macrobicycle **L1** having N4 cavity (Figure 1) can form four/five coordinated complex with Pd^{II}.[18] Thus, it would be interesting to explore the selectivity of the Pd^{II} complex of **L1** towards C–C coupling reactions. Importantly, the ethynyl iodo group is found to be an efficient halogen-bond donor, having significant σ-hole potential towards lone pair rich halogen bond acceptors.[19] Whereas, oxygen is a well-established acceptor for the halogen bonding interaction due to its easy availability of lone pair of electrons.[20] Thus, **L1**, having a distinct 3D oxy-ether pocket, might favour a selective interaction with the ethynyl iodide. Therefore, the Suzuki coupling is surveyed of a substrate 1- iodoethynyl-4-iodobenzene, **1a**, having two different labile C–I bonds (aryl iodo and ethynyl iodo groups). A suitable oxy-ether pocket as well as three well-organized benzene in the framework of **L1** might induce π–π stacking interaction effectively to bind aryl iodo end of **1a** to Pd^{II} center selectively.

Consequently, the aryl iodo part of **1a** can go through the site selective Suzuki coupling with arylboronic acid keeping ethynyl iodo part intact from organoborons. To find out the effect of three dimensional macrobicyclic cavity of **L1**, its acyclic analog,[15] **L′** (Figure 1) has also been explored. Furthermore, to verify the effect of dimension of the macrobicycle cage, an analogous macrobicycle of **L1** having smaller cavity size, **L2** (Figure 1, Scheme 1 S, Supporting Information) has also been synthesized.

Optimization of the reaction conditions

To investigate the effect of **L1** toward the Pd^{II} catalysed coupling reaction, **1a** and phenylboronic acid **2a** have been chosen as model substrates. Since only one Pd^{II} binding site is present in **L1**, equimolar mixture of Pd^{II} catalyst and **L1** (1:1) is used for the above studies. Firstly, the reaction conditions have been optimized toward the effective production of 1,3-diyne **3a** in high yield. The catalytic activity of various Pd^{II} salts such as $Pd(OAc)_2$, $Pd(NO_3)_2$ and $PdCl_2$ have been screened upon varying time as well as temperature (Table 1). Among different solvent systems (Table 1, entries 4–8) CH_3OH and DMSO have been resulted the higher yields (67–68%) where CH_3OH has been preferred for its greater sustainability. Remarkably, ethynyl iodo part does not react with the organoboron (**2a**), even at higher temperature and with longer reaction time (Table 1, entries 13,14). When different bases are explored, K_2CO_3 has shown greater capability towards efficient product formation. To determine the amount of Pd^{II}-**L1** mixture required for the reaction of **1a** and **2a**, various amounts of 1:1 mixture of Pd^{II} and **L1** are attempted (Figure 2). A linear increase in the yield upto 10 mol% is observed for the effective percentage of the mixture.

Table 1. Optimization of the reaction conditions.[a]

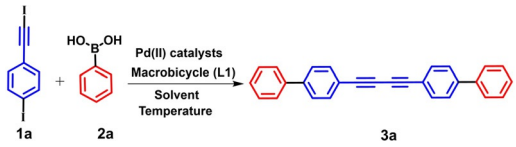

Entry	Catalyst	Solvent	Base	*T* [°C]	*t* [h]	Yield [%][b]
1	$Pd(OAc)_2$	CH_3OH	K_2CO_3	60	24	35
2	Pd_2dba_3	CH_3OH	K_2CO_3	60	24	28
3	$Pd(NO_3)_2$	CH_3OH	K_2CO_3	60	12	31
4	$PdCl_2$	CH_3OH	K_2CO_3	60	5	68
5	$PdCl_2$	DMSO	K_2CO_3	60	5	67
6	$PdCl_2$	DMF	K_2CO_3	80	8	27
7	$PdCl_2$	CH_3CN	K_2CO_3	80	8	20
8	$PdCl_2$	C_2H_5OH	K_2CO_3	60	10	25
9	$PdCl_2$	CH_3OH	Na_2CO_3	60	12	52
10	$PdCl_2$	CH_3OH	Cs_2CO_3	60	12	48
11	$PdCl_2$	CH_3OH	NEt_3	60	12	21
12	$PdCl_2$	CH_3OH	K_2CO_3	50	12	57
13	$PdCl_2$	CH_3OH	K_2CO_3	60	24	67
14	$PdCl_2$	DMSO	K_2CO_3	100	24	66

[a] The reaction was performed using **1a** (1.0 mmol), phenylboronic acid **2a** (1.3 mmol), catalyst (10 mol%), base (2.0 mmol) and **L1** (10 mol%) in 2 mL solvent under argon atmosphere. [b] Isolated yields.

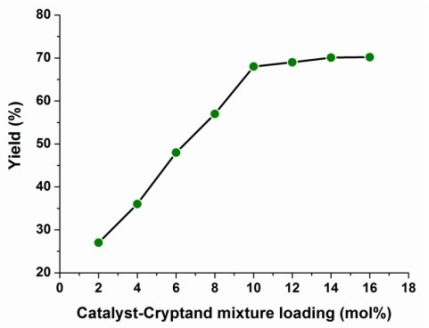

Figure 2. Survey of yield (%) vs. catalyst-cryptand mixture loading (mol%).

In this regard, use of Pd^0 salt as catalyst is found to be ineffective towards the desired regioselective product formation (Table 1, entry 2), which could be due to poor/non-complexing ability of Pd^0 with **L1**.

To understand the effect of cage structure of **L1** in the coupling reaction, acyclic analog of **L1** that is, **L′** is explored. In optimized condition, **3a** has only been produced as the minor product over dual Suzuki coupling product, **4a** (Table 2, entry 1) when **L1** is replaced by **L′**. This could be due to the flexibility of tripodal arms of **L′**, which is unable to protect the ethynyl iodo group from **2a**. Furthermore, to check the effect

Table 2. Comparative reaction study using different additives.[a]

Entry	Additive	Yield of **3a** [%][b]	Yield of **4a** [%][b]
1	L′	11	40
2	**L2**	12	35
3	DB18C6	8	41
4	–	8	43
5	**L1**	68	6

[a] The reaction was performed using **1a** (1.0 mmol), **2a** (1.3 mmol), catalyst (10 mol%), base (2.0 mmol) and additive (10 mol%) in 2 mL solvent under argon atmosphere. [b] Isolated yields.

of cage dimension, a cryptand with smaller cavity, **L2**, is further explored as an additive under optimized reaction conditions. However, it fails to produce **3a** substantially and only a minor amount (12%) is obtained (Table 2, entry 2).

When Dibenzo-18-crown-6 (DB18C6) is used as additive, **3a** is found to be the minor product (Table 2, entry 3). Most importantly, when a simple Pd^{II} salt ($PdCl_2$) is used as catalyst for this reaction (Table 2, entry 4), insignificant amount of **3a** (8%) has been isolated. Thus, effect of rigidity (macrobicyclic versus acyclic tripodal), cavity dimensions of different macrobicycles and simple Pd^{II} salt versus Pd^{II}-cryptate as catalyst typically prove that suitable 3D cavity of **L1** and its Pd^{II} complex are very crucial for the protection of ethynyl iodo to produce **3a** as the main product (Table 2, entry 5).

Thus, the above reaction method can be generalized as a cascade C–C coupling process involving site selective Suzuki coupling of aryl iodide followed by the tandem homocoupling of ethynyl iodo part as an inevitable effect of the reaction medium.

Substrate scope

At the optimized reaction condition, various aromatic boronic acids have been reacted with **1a** to produce nine dual coupling products (**3a–i**, Scheme 2). All the products have been thoroughly characterized by NMR (Figure S2–S19, Supporting Information), IR and HRMS. Scheme 2 clearly demonstrates that the reaction of different arylboronic acids and **1a** has a generalized impact towards the dual coupling product 1,3-diynes formation. Electron donating aryl boronic acids reacts more prominently with $C(sp^2)$ atom of **1a** to form finally the 1,3 diyne products with better yields (**3b–g**).

However, electron withdrawing boronic acids have produced relatively poor yields of 1,3-diyne products (**3h–i**) because of its greater self-coupling tendency by performing efficient deborylation. Importantly, we have been successful to crystalize two of the products **3c** and **3i**, where both the single-crystal X-ray diffraction structural analyses have confirmed the formation of 1,3-diynes (Figure 3).

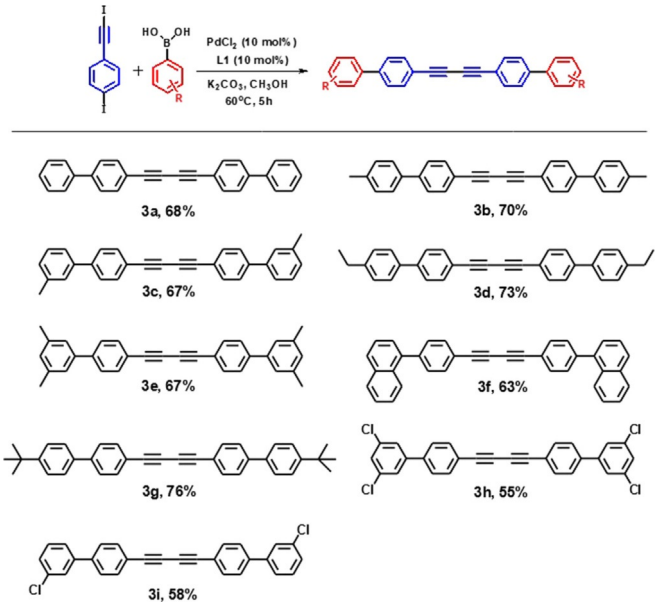

Scheme 2. List of synthesized symmetrical 1,3-diynes. Reactions were carried out using **1a** (1.0 mmol), arylboronic acids (1.3 mmol), catalyst (10 mol%), base (2.0 mmol) and **L1** (10 mol%) in 2 mL CH_3OH under argon atmosphere. Isolated yields.

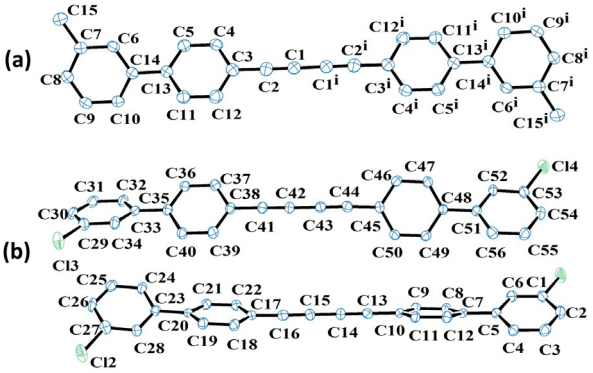

Figure 3. ORTEP plot of (a) compound **3c** and (b) compound **3i** [50% Probability].

Scope in dual heterocoupling

We have extended the viability of this reaction procedure by adding different ethynyl iodo derivatives **5a–d** (Scheme 3) to the reaction mixture after 30 min of initialization to observe the one pot site selective dual C–C bond forming heterocoupling reactions. Remarkably, unsymmetrical 1,3-diynes have been formed in considerable yields (Figures S22–S29, Supporting Information). Thus, this event creates an opportunity for the one-pot cross $C(sp^2)$–$C(sp^2)$ coupling plus cross C(sp)–C(sp) coupling under optimized reaction conditions.

Insight into the cascade dual C–C coupling

It can be emphasized that for the effective formation of 1,3-diyne products, Pd^{II} catalyzed reaction of **1a** and arylboronic acids in presence of macrobicycle **L1** must prefer a particular

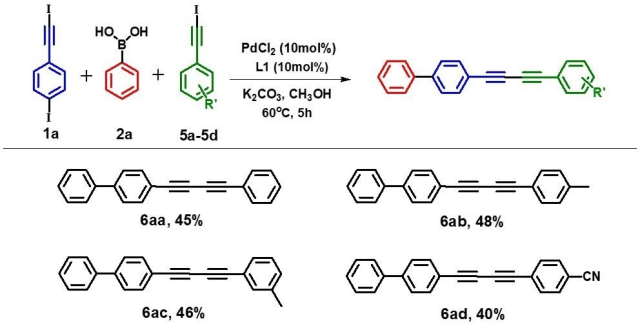

Scheme 3. List of synthesized unsymmetrical 1,3-diynes.Reactions were carried out using **1a** (1.0 mmol), **2a** (1.0 mmol), **5a–5d** (1.0 mmol), catalyst (10 mol%), base (2.0 mmol) and **L1** (10 mol%) in 2 mL CH_3OH under argon conditions. Isolated yields.

pathway among different possibilities of competitive C–C coupling reactions (Scheme 4). Thus, to get insight into the **L1** assisted Pd^{II} catalyzed cascade dual C–C coupling reaction between **1a** and **2a**, a systematic investigation have been carried out. Upon reacting **L1** with $PdCl_2$ in CH_3OH for 10 min, a characteristic peak at m/Z 941.31 is observed in the ESI-MS (Figure S34, Supporting Information), which indicates the formation of [**L1**-Pd(Cl)]$^+$ (Species I, Scheme S2, Supporting Information) in the system. Complexation of Pd^{II} with **L1** is further evident from the splitting of all the aromatic protons of **L1** due of the change in the chemical environment. ^{1}H NMR splitting pattern indicates that the complex is dissymmetric in nature, having four coordinated square planar geometry around Pd^{II} center in the tris-amine pocket of **L1**.[18] Furthermore, the DOSY-NMR spectrum (Figure S37, Supporting Information) of the mixture shows a similar diffusion coefficient values of all the assigned peaks. Fitting of the amplitude decay of all the selected peaks to the mono-exponential function (Figure S38, Supporting Information) has clearly shown comparable decay constants along with similar residuals. These results confirmed the existence of only one type of complex in the solution.[21]

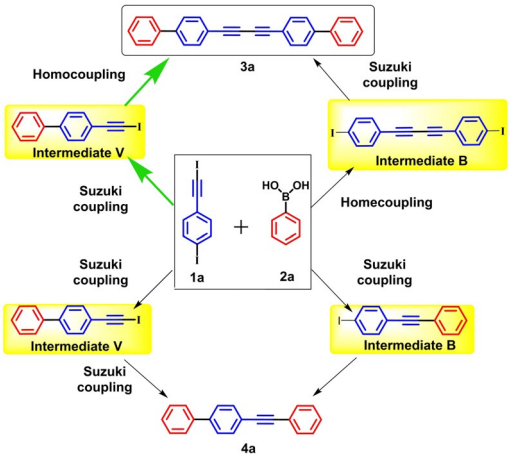

Scheme 4. Different possible cascade C–C coupling reactions involving various potential intermediates; Green arrows indicate the macrobicycle assisted cascade reaction pathway.

When the species I is further reacted with **1a**, **2a** and K_2CO_3 for 30 min in reflux condition, the ESI-MS of the crude reaction mixture shows a peak at m/Z 1205.21 (Figure S35, Supporting Information), which corresponds to [**L1**-Pd(C_6H_4C≡C-I)(Cl)]$^+$ (Species III, Scheme S2, Supporting Information). The formation of species III in the above reaction condition could be explained by simultaneous reduction of Pd^{II} center (Species I) to Pd^0 (Species II) and oxidative addition of **1a** to Pd^0 preferably via breaking of the Ar-I bond. Further, the encapsulation of **1a** through cascade complexation in the cavity of Pd^{II}-**L1** cryptate has been confirmed by a comparative ^{1}H NMR studies of **L1**, **L1**-$PdCl_2$ (1:1 mixture at 60 °C) and **L1**-$PdCl_2$-**1a** (1:1:1 basic mixture at 60 °C) (Figures S39–S44, Supporting Information). When equimolar amount of **1a** is added to the in situ **L1**-Pd^{II} complex in presence of K_2CO_3 and upon heating at 60 °C, the aromatic protons of **1a** shifts to the downfield region ($\Delta\delta \approx 0.15$ and ≈ 0.08 ppm), which could be due to suitable π–π stacking interaction between aromatic moieties of **1a** and **L1**-Pd^{II} cryptate upon cascade complex formation. ^{13}C NMR peak shift of C–I carbon in the presence of halogen bond acceptor atoms depicts probable halogen bonding interaction and is well described in recent literatures.[22] Therefore, to verify the halogen bonding interaction of ethynyl iodo group inside the oxyether pocket of **L1**, we have performed comparative ^{13}C NMR spectral studies (Figure S55, Supporting Information) of **1a** with 1:1:1 basic mixture of **L1**, Pd^{II} and **1a** which shows that the peak of the ethynyl carbon atom (C_α) of **1a** attached to the iodo group has been significantly shifted ($\Delta\delta \approx 1.7$ ppm). The next carbon (C_β) is also shifted to some extent ($\Delta\delta \approx 0.3$ ppm). This indicates potential halogen bonding interaction of ethynyl iodide with the oxy-ether pocket of **L1**. Consequently, all of these facts rules out the formation of Intermediate **A** or Intermediate **B** (Scheme 4) during the course of the reaction, as the formation of those intermediates entirely depend on the initial breaking of the ethynyl iodo bond of **1a**.

Finally, when phenylboronic acid **2a** undergoes reaction with the species III, a transmetalation reaction at the Pd^{II} center probably taking place to form the species IV, which further undergoes reductive elimination of C(sp^2)–C(sp^2) coupling product **V** to regenerate the species II having Pd^0 center (Scheme S2, Supporting Information). Finally, ethynyl iodo intermediate **V** undergoes a C(sp)–C(sp) homocoupling reaction to form 1,3-diyne **3a** in considerable yields, catalyzed by species II.

To exactly determine the proper series of cascade reaction, detection of the intermediate is indeed important. Thus the existence of the particular intermediate in the mechanistic pathway has been verified by quenching the reaction mixture after 1 h. Upon purification it has been observed that the intermediate **V** is being produced during the course of this reaction. Furthermore, as a support, we have attempted to trap the intermediate **V** by reacting with benzyl azide and CuI for 30 min (Scheme 5). A peak at *m/z* 460.04 in the ESI-MS of the crude indicates the formation of 5-iodotriazole **2b** (Figure S52, Supporting Information). Hence, this confirms that the course of this macrobicycle assisted cascade C–C coupling is following

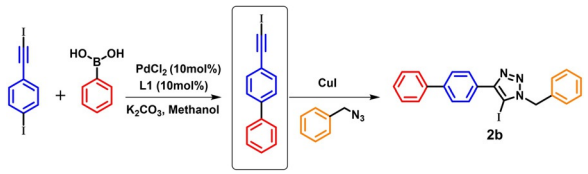

Scheme 5. Formation of 5-iodotriazole derivative.

the transformation from **1a** to intermediate **V** followed by homocoupling of intermediate **V** to **3a** (Scheme 4, green arrows).

To support the involvement of **L1**-$PdCl_2$ complex in this homocoupling reaction, separate homocoupling reactions of 1-(Iodoethynyl) benzene and intermediate **V** in the presence of **L1**-$PdCl_2$ in situ complex are studied which has eventually yielded affordable C–C coupling products (Table 3).

Moreover, to rationalize the existence of Pd^{II}/Pd^{0} in the catalytic cycle, **L1**-$PdCl_2$ complex is heated in methanol for 15 min in presence of K_2CO_3 and the ESI-MS (positive ion mode) of this mixture shows a peak at 906.34 which corresponds to [**L1**-Pd]$^+$ species (Figure S36, Supporting Information). This could be due to the presence of Pd^0 species in the mixture which is originated upon reduction of Pd^{II} species in the presence of a base in suitable solvent.[23]

Table 3. Homocoupling study.[a]

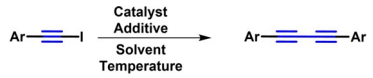

Entry	Substrate	Product	Yield [%][b]
1		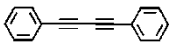 **10**	81
2	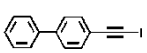	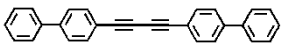 **3a**	78

[a] The reactions were carried out using substrates (0.5 mmol), $PdCl_2$ catalyst (10 mol%), **L1** (10 mol%) and K_2CO_3 (1.0 mmol) in 2 mL CH_3OH under argon atmosphere for 5 h. [b] Isolated yields.

Kinetic aspects of the cascade dual C–C coupling

Furthermore, the proposed mechanism has been substantiated by the time dependent kinetic studies in optical spectroscopy. The optimized reaction of **1a** with **2a** in the presence of **L1**-Pd complex has been monitored by observing the appearance of **3a** with time. For the initial 200 s of the reaction, the characteristic absorption maxima of **3a** at 340 nm does not appear. After 200 s, the peak at 340 nm begins to form and increases following a pseudo-first order kinetics with a rate of $3.2\times10^{-4}\,M^{-1}s^{-1}$ (Figure 4 and Figure S45, Supporting Information).

This observation clearly establishes that a lag phase of 200 s exists before the formation of **3a**. In this lag phase, the intermediate **V** is possibly forming by the faster Suzuki coupling of aryl iodo group, which initializes the homocoupling of ethynyl iodo group towards the formation of **3a** after 200 s. On the contrary, the pseudo-first order kinetics for the formation of **3a**

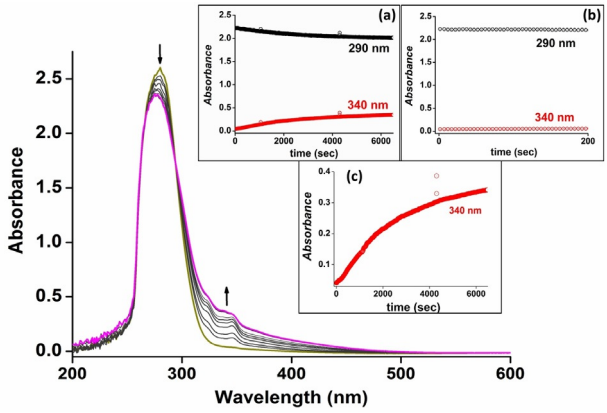

Figure 4. Time-dependent formation of **3a** by the reaction of **1a** and **2a** under optimized conditions. Inset pictures represent (a) change of absorbance at 290 nm and 340 nm with time, (b) change of absorbance at 290 and 340 nm within 200 s, (c) change in absorbance at 340 nm with time.

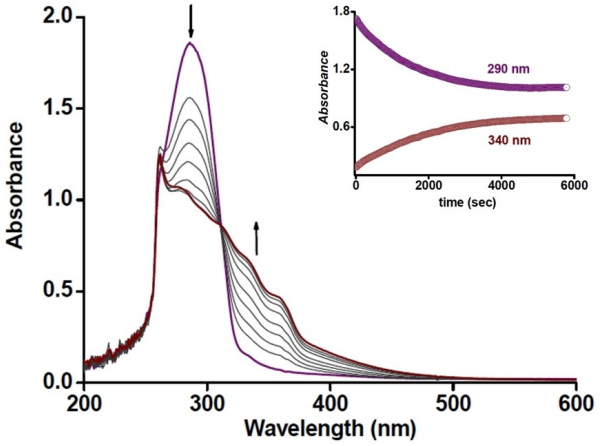

Figure 5. Time-dependent formation of **3a** by the homocoupling of Intermediate **V** under optimized condition.

by the homocoupling of intermediate **V** in presence of **L1**-Pd complex has also been observed. In this case the rate of the reaction is found to be $4.8\times10^{-4}\,M^{-1}s^{-1}$ (Figure 5 and Figure S46, Supporting Information).

Almost comparable rates of these two reactions have clearly pointed out that the formation of **3a** from intermediate **V** is the slowest step in the optimized two-step transformation of **1a** to **3a**. The faster rate of formation of intermediate **V** from **1a** is probably due to the noncovalent interactions of **1a** (protective halogen bonding and π–π stacking interaction) with the cage. This interaction assists the substrate **1a** in such a way that aryl iodo group becomes closer to the metal center which thereby facilitates faster attack of boronic acid to this C(sp^2)–X group. After the formation of intermediate **V**, it comes out from the macrobicycle and performs slower homocoupling reaction of ethynyl iodo group to form **3a**. Finally to rationalize the importance of the macrobicycle **L1** for this dual coupling, some cross experiments have been incorporated via kinetic measurements. Reaction of simple trimethylsilyl protected ethynyl-4-iodobenzene with phenylboronic acid in presence

of only $PdCl_2$ salt shows a slower reaction kinetics (Figure S48, Supporting Information) where the substrate does not reach the equilibrium even after 10000 s. Also, the homocoupling of 1-(iodoethynyl)benzene does not even occurred in presence of only $PdCl_2$ catalyst (Figure S49, Supporting Information). These reactions have clearly shown that in absence of **L1**, $PdCl_2$ catalyzed Suzuki coupling of aryl iodo group and homocoupling of ethynyl iodo functionality are not substantial reactions to achieve. From all these kinetic experiments it can be anticipated that employment of **L1** thus not only imposes the selectivity of aryl iodo group towards Suzuki coupling over ethynyl iodo functionality, but also increases the feasibility of both the C–C coupling reactions.

Conclusions

In summary, we have designed a heteroditopic macrobicycle-Pd^{II} complex catalyzed one-pot synthetic route for preparing 1,3-diynes by site selective Suzuki coupling of aryl iodo groups with arylboronic acids and sequential homocoupling of the ethynyl iodo functionality of a single substrate. Protection of ethynyl iodo group from arylboronic acids has been imparted probably due to protective halogen-bonding interaction of ethynyl iodide with the oxy-ether pocket of macrobicycle. Moreover, the scope of this approach has been extended by the novel preparation of unsymmetrical 1,3-diynes with excellent yields. Furthermore, kinetic aspects of this multistep reaction have also been studied. Exploitation of macrobicycles for selective C–C coupling reactions may advance recent synthetic methods in near future.

Experimental Section

General details

All the starting materials were purchased from commercial sources such as Sigma Aldrich, Merck, Spectrochem and Alfa Aesar and are used as received without further purification. Compound **1a** was synthesized using previously reported procedure.[24] Iodoalkynes **5a**, **5b**, **5c** and **5d** were synthesized by following the previously reported general procedure.[25] Detailed synthetic method for the preparation of Macrobicycle **L2** has been described in Supporting Information File. **L1** and **L′** were synthesized according to the previous literature report.[15] Melting points of all the compounds were determined on a Labtronics digital auto melting/boiling point apparatus. Solution electronic spectra (single and time-dependent) were measured on an Agilent 8453 diode array spectrophotometer. IR data was recorded on a SHIMADZU FTIR-8400S Infrared spectrophotometer. All the NMR experiments were obtained on 300, 400 and 500 MHz Bruker DPX. For DOSY-NMR data, the fit of the amplitude decay for selected peaks to the mono-exponential function has been processed using GNAT (General NMR Analysis Toolbox) software (https://www.nmr.chemistry.manchester.ac.uk/?q=node/430).

General procedure for synthesis of symmetrical 1,3-diynes (3a–3i)

In a 10 mL round bottom flask macrobicycle **L1** (10 mol%) and $PdCl_2$ (10 mol%) was mixed in CH_3OH and stirred for 10 min. 1-iodoethynyl-4-iodobenzene **1a** (1 mmol), arylboronic acids (1.3 mmol) and K_2CO_3 (2 mmol) were then added and overall reaction mixture was allowed to stir for another 5 h at 60 °C. Then the crude was filtered and solvent of the filtrate was evaporated and all the products were purified by preparative thin layer chromatography.

General procedure for synthesis of unsymmetrical 1,3-diynes (6aa–6ad)

In a 10 mL round bottom flask macrobicycle **L1** (10 mol%) and $PdCl_2$ (10 mol%) was mixed in CH_3OH and stirred for 10 min. 1-iodoethynyl-4-iodobenzene, **1a** (1 mmol), phenylboronic acids (1 mmol), and K_2CO_3 (2 mmol) were then added and allowed to stir at 60 °C. After 30 min, ethynyl iodo derivatives **5a**–**5d** (1 mmol) was added to the reaction mixture. Overall reaction mixture was allowed to stir for another 5 h at 60 °C. Then the crude was filtered and solvent of the filtrate was evaporated and all the products were purified by preparative thin layer chromatography.

X-ray crystallographic refinement details

X-ray quality single crystals of **compound 3c** and **compound 3i** were obtained by slow evaporation of $CHCl_3$ solution of the compounds. Single crystal X-ray diffraction data were collected using Bruker APEX III D8 Venture, PHOTON II detector ($Mo_{K\alpha}$, λ = 0.7107 Å). Data collection, data reduction, structure solution and refinement were carried out using the software package of the corresponding diffractometer. All the structures were solved by direct methods and refined in a routine manner. Hydrogen atoms were geometrically fixed. All the non-hydrogen atoms were treated anisotropically. Deposition numbers 2020012 (for **3c**) and 2020013 (for **3i**) contain the supplementary crystallographic data for this paper. These data are provided free of charge by the joint Cambridge Crystallographic Data Centre and Fachinformationszentrum Karlsruhe Access Structures service www.ccdc.cam.ac.uk/structures.

Characterization data

1,4-bis(4-biphenyl)buta-1,3-diyne (3a): Yellowish solid (241 mg, 68%), purified by column chromatography (eluent: hexane), mp: 242 °C; IR (KBr): $\tilde{\nu}$ = 2925, 2854, 1741, 1461, 837, 757 cm^{-1}; ^1H NMR (400 MHz, $CDCl_3$): δ = 7.37 (t, J = 7.2 Hz, 2H), 7.46 (t, J = 7.4 Hz, 4H), 7.57–7.62 ppm (m, 12H); ^{13}C NMR (100 MHz, $CDCl_3$): 74.8, 82.0, 120.8, 127.2, 127.3, 128.0, 129.1, 133.1, 140.3, 142.2; HRMS (EI) m/z: M^+ Calcd for $[C_{28}H_{18}]$: 354.1408, Found 354.1410.

1,4-bis(4′-methyl-4-biphenyl)buta-1,3-diyne (3b): White solid (267 mg, 70%), purified by column chromatography (eluent: hexane), mp: >250 °C; IR (KBr): $\tilde{\nu}$ = 2923, 2852, 1741, 1463, 1377, 812 cm^{-1}; ^1H NMR (500 MHz, $CDCl_3$): 2.40 (s, 6H), 7.27 (s, 2H), 7.49–7.52 (m, 6H), 7.55–7.60 (m, 8H); ^{13}C NMR (100 MHz, $CDCl_3$): 21.3, 74.7, 82.0, 120.5, 127.0, 129.8, 133.1, 137.4, 138.0, 142.0; HRMS (EI) m/z: M^+ Calcd for $[C_{30}H_{22}]$: 382.1721, Found 382.1720.

1,4-bis(3′-methyl-4-biphenyl)buta-1,3-diyne (3c): Pale yellow solid (256 mg, 67%), purified by column chromatography (eluent: hexane), mp: 182 °C; IR (KBr): $\tilde{\nu}$ = 2923, 2852, 2146, 1600, 1479, 1375, 835, 738 cm^{-1}; ^1H NMR (500 MHz, $CDCl_3$): 2.43 (s, 6H), 7.19 (d, J = 7 Hz, 2H), 7.33–7.43 (m, 6H), 7.56–7.61 (m, 8H); ^{13}C NMR (100 MHz, $CDCl_3$): 21.7, 74.8, 82.0, 120.7, 124.3, 127.3, 128.0, 128.8, 129.0, 133.0, 138.7, 140.2, 142.3; HRMS (EI) m/z: M^+ Calcd for $[C_{30}H_{22}]$: 383.1721, Found 383.1718.

1,4-bis(4′-ethyl-4-biphenyl)buta-1,3-diyne (3d): White solid (299 mg, 73%), purified by column chromatography (eluent:

hexane), mp: 240 °C; IR (KBr): $\tilde{\nu}$ = 2924, 2880, 2142, 1603, 1482, 820 cm^{-1}; ^{1}H NMR (500 MHz, $CDCl_3$): 1.28 (t, J = 7.8 Hz, 6H), 2.70 (q, J = 7.6 Hz, 4H,), 7.29 (d, J = 8.0 Hz, 4H), 7.52 (d, J = 8.0 Hz, 4H), 7.56–7.60 (m, 8H). ^{13}C NMR (100 MHz, $CDCl_3$): 15.6, 28.7, 74.8, 82.1, 120.5, 127.1, 127.1, 128.6, 133.1, 137.6, 142.1, 144.3; HRMS (EI) *m/z*: M^+ Calcd for [$C_{32}H_{26}$]: 410.2035, Found 410.2040.

1,4-bis(3′,5′-dimethyl-4-biphenyl)buta-1,3-diyne (3 e): White solid (274 mg, 67%), purified by column chromatography (eluent: hexane), mp: > 250 °C; IR (KBr): $\tilde{\nu}$ = 2924, 2860, 1595, 1478, 1381, 832, 742 cm^{-1}; ^{1}H NMR (500 MHz, $CDCl_3$): 2.31 (s, 12H), 6.98 (s, 2H), 7.22–7.24 (m, 6H), 7.67–7.70 (m, 6H); ^{13}C NMR (100 MHz, $CDCl_3$): 21.2, 75.3, 81.4, 121.3, 129.4, 130.6, 133.2, 134.0, 137.6, 137.9, 138.1; HRMS (EI) *m/z*: M^+ Calcd for [$C_{32}H_{26}$]: 410.2035, Found 410.2038.

1,4-bis[4-(2-naphthyl)-phenyl]buta-1,3-diyne (3 f): Pale yellow solid (286 mg, 63%), purified by column chromatography (eluent: 2% ethyl acetate in hexane), mp: 208 °C; IR (KBr): $\tilde{\nu}$ = 2923, 2852, 1585, 1382, 800, 781 cm^{-1}; ^{1}H NMR (500 MHz, $CDCl_3$): 7.24 (d, J = 8.5 Hz, 1H), 7.29 (t, J = 7.8 Hz, 3H), 7.40 (d, J = 8.5 Hz, 2H), 7.46–7.50 (m, 6H), 7.60 (t, J = 7.5 Hz, 3H), 7.69 (d, J = 8.5 Hz, 1H), 7.94–7.96 (m, 6H); ^{13}C NMR (125 MHz, $CDCl_3$): 75.2, 81.4, 121.3, 125.5, 125.9, 126.1, 126.7, 128.0, 128.0, 128.3, 133.0, 133.7, 134.0, 137.9, 138.6, 139.4; HRMS (EI) *m/z*: M^+ Calcd for [$C_{36}H_{22}$]: 454.1721, Found 454.1718.

1,4-bis(4′-tert-butyl-4-biphenyl)buta-1,3-diyne (3 g): White solid (354 mg, 76%), purified by column chromatography (eluent: hexane), mp: > 250 °C; IR (KBr): $\tilde{\nu}$ = 2836, 2142, 1577, 1490, 1250, 820 cm^{-1}; ^{1}H NMR (400 MHz, $CDCl_3$): 1.36 (s, 18H), 7.48 (d, J = 8.8 Hz, 4H) 7.51–7.61 (m, 12H); ^{13}C NMR (75 MHz,$CDCl_3$): 31.5, 34.8, 74.7, 82.0, 120.5, 126.0, 126.8, 127.1, 133.1, 137.3, 141.9; HRMS (EI) *m/z*: M^+ Calcd for [$C_{36}H_{34}$]: 466.2661, Found 466.2665.

1,4-bis(3′,5′-dichloro-4-biphenyl)buta-1,3-diyne (3 h): White solid (270 mg, 55%), purified by column chromatography (eluent: hexane), mp: 190 °C; IR (KBr): $\tilde{\nu}$ = 2958, 2852, 2198, 1238, 820, 790 cm^{-1}; ^{1}H NMR (400 MHz, $CDCl_3$): 7.36–7.37 (m, 2H), 7.46–7.46 (m, 4H), 7.51–7.54 (m, 4H), 7.60–7.63 (m, 4H); ^{13}C NMR (100 MHz, $CDCl_3$): 75.4, 81.8, 122.1, 125.7, 127.3, 127.9, 133.3, 135.7, 139.4, 143.2; HRMS (EI) *m/z*: M^+ Calcd for [$C_{28}H_{14}Cl_4$]: 489.9824, Found 489.9819.

1,4-bis(3′-chloro-4-biphenyl)buta-1,3-diyne (3 i): Pale yellow solid (245 mg, 58%), purified by column chromatography (eluent: hexane), mp: 185 °C; IR (KBr): $\tilde{\nu}$ = 3012, 2280, 1234, 1155, 822, 753 cm^{-1}; ^{1}H NMR (500 MHz, $CDCl_3$): 7.34–7.40 (m, 4H), 7.47 (d, J = 7.5 Hz, 2H), 7.55–7.58 (m, 6H), 7.62 (d, J = 8.0 Hz, 4H); ^{13}C NMR (125 MHz, $CDCl_3$): 75.1, 81.9, 121.5, 125.4, 127.3, 127.4, 128.0, 130.3, 133.2, 135.0, 140.7, 142.1; HRMS (EI) *m/z*: M^+ Calcd for [$C_{28}H_{16}Cl_2$]: 422.0629, Found 422.0632.

4-(Phenylethynyl)-1,1′-biphenyl (4 a): White solid, purified by column chromatography (Eluent: hexane), mp: 165 °C; IR (KBr): $\tilde{\nu}$ = 3061, 3032, 1901, 1441, 1404, 1180, 1065 cm^{-1}; ^{1}H NMR (400 MHz, $CDCl_3$): 7.35–7.38 (m, 4H), 7.44–7.48 (m, 2H), 7.54–7.62 (m, 8H); ^{13}C NMR (100 MHz, $CDCl_3$): 89.5, 90.2, 122.4, 123.5, 127.2, 127.8, 128.4, 128.5, 129.0, 131.8, 132.2, 140.5, 141.1; HRMS (EI) *m/z*: M^+ Calcd for [$C_{20}H_{14}$]: 254.1096, Found 254.1095.

4-(4-Phenylbuta-1,3-diyn-1-yl)biphenyl (6 aa): White solid (125 mg, 45%), purified by column chromatography (eluent: hexane), mp: 155 °C; IR (KBr): $\tilde{\nu}$ = 2920, 2146, 1596, 1481, 1004, 841, 754 cm^{-1}; ^{1}H NMR (400 MHz, $CDCl_3$): 7.33–7.39 (m, 4H), 7.46 (t, J = 7.6 Hz, 2H), 7.53–7.62 (m, 8H); ^{13}C NMR (125 MHz, $CDCl_3$): 74.2, 74.7, 81.7, 82.0, 120.8, 122.0, 127.2, 127.3, 128.0, 128.6, 129.1, 129.4, 132.7, 133.1, 140.3, 142.1; HRMS (EI) *m/z*: M^+ Calcd for [$C_{22}H_{14}$]: 278.1096, Found 278.1099.

4-[4-(4-methylphenyl)buta-1,3-diyn-1-yl]biphenyl (6 ab): White solid (140 mg, 48%), purified by column chromatography (eluent: hexane), mp: 161 °C; IR (KBr): $\tilde{\nu}$ = 2920, 2360, 1598, 1485, 1020, 840, 761, 694 cm^{-1}; ^{1}H NMR (400 MHz, $CDCl_3$): 2.37 (s, 3H), 7.15 (d, J = 8.0 Hz, 2H), 7.37 (t, J = 7.2 Hz, 1H), 7.42–7.47 (m, 4H), 7.56–7.61 (m, 6H); ^{13}C NMR (100 MHz, $CDCl_3$): 21.8, 73.6, 74.9, 81.4, 82.4, 118.9, 121.0, 127.2, 127.3, 128.0, 129.1, 129.4, 132.6, 133.1, 139.8, 140.3, 142.0; HRMS (EI) *m/z*: M^+ Calcd for [$C_{23}H_{16}$]: 292.1252, Found 292.1250.

4-[4-(3-methylphenyl)buta-1,3-diyn-1-yl]biphenyl (6 ac): Pale yellow solid (134 mg, 46%), purified by column chromatography (eluent: hexane), mp: 152 °C; IR (KBr): $\tilde{\nu}$ = 2921, 2850, 2142, 1598, 1481, 1006, 840, 784, 765, 686 cm^{-1}; ^{1}H NMR (400 MHz, $CDCl_3$): 2.35 (s, 3H), 7.18–7.24 (m, 2H), 7.34–7.39 (m, 3H), 7.46 (t, J = 7.6 Hz, 2H), 7.58–7.61 (m, 6H); ^{13}C NMR (100 MHz, $CDCl_3$): 21.3, 73.8, 74.8, 81.5, 82.3, 120.9, 121.8, 127.2, 127.3, 128.0, 128.5, 129.1, 129.8, 130.3, 133.1, 133.2, 138.4, 140.3, 142.1; HRMS (EI) *m/z*: M^+ Calcd for [$C_{23}H_{16}$]: 292.1252, Found 292.1256.

4-[4-(4-cyanophenyl)buta-1,3-diyn-1-yl]biphenyl (6 ad): White solid (121 mg, 40%), purified by column chromatography (eluent: 2% ethyl acetate in hexane), mp: 188 °C; IR (KBr): $\tilde{\nu}$ = 2920, 2850, 2229, 2216, 1598, 1483, 1402, 1269, 1105, 837, 767, 703 cm^{-1}; ^{1}H NMR (400 MHz, $CDCl_3$): 7.36–7.40 (m, 1H), 7.44–7.48 (m, 2H), 7.58–7.65 (m, 10H); ^{13}C NMR (100 MHz, $CDCl_3$): 74.1, 78.4, 79.8, 84.1, 112.6, 118.4, 120.1, 127.1, 127.2, 127.4, 128.2, 129.1, 132.1, 132.3, 133.1, 133.2, 140.1, 142.7; HRMS (EI) *m/z*: M^+ Calcd for [$C_{23}H_{13}N$]: 303.1048, Found 303.1050.

Compound 10: White solid, purified by column chromatography (Eluent: hexane); ^{1}H NMR (300 MHz, $CDCl_3$): 7.31–7.40 (m, 6H), 7.54 (d, J = 6.6 Hz, 4H); ^{13}C NMR (75 MHz, $CDCl_3$): 74.1, 81.7, 121.9, 128.6, 129.3, 132.7; HRMS (EI) *m/z*: M^+ Calcd for [$C_{16}H_{10}$]: 202.0782, Found 202.0780.

Acknowledgements

P.G. gratefully acknowledges the Science and Engineering Research Board (SERB; CRG/2019/002236), India, for financial support. S.S. and S.M. thank Council for Scientific and Industrial Research (CSIR, New Delhi) for their fellowship (SRF). P.S. thanks the SERB project CRG/2019/002236 for her fellowship (RA). The authors also thank Indian Association for the Cultivation of Science (IACS, Kolkata) for the Instrumentation Facility.

Conflict of interest

The authors declare no conflict of interest.

Keywords: 1,3-diyne · C–C coupling · macrobicycle · regioselectivity · supramolecular catalysis

[1] a) N. Miyaura, A. Suzuki, *Chem. Rev.* **1995**, *95*, 2457–2483; b) A. Suzuki, *Chem. Commun.* **2005**, 4759–4763; c) "Catalytic Asymmetric Suzuki–Miyaura Couplings": F. W. Goetzke, L. V. Dijk, S. P. Fletcher in *PATAI'S Chemistry of Functional Groups*, (Ed.: Z. Rappoport), Wiley, **2019**; d) S. E. Hooshmand, B. Heidari, R. Sedghi, R. S. Varma, *Green Chem.* **2019**, *21*, 381–405; e) R. Martin, S. L. Buchwald, *Acc. Chem. Res.* **2008**, *41*, 1461–1473; f) J. P. G. Rygus, C. M. Crudden, *J. Am. Chem. Soc.* **2017**, *139*, 18124–18137.

[2] a) S. R. Chemler, D. Trauner, S. J. Danishefsky, *Angew. Chem. Int. Ed.* **2001**, *40*, 4544–4568; *Angew. Chem.* **2001**, *113*, 4676–4701; b) R. J.

Procter, J. J. Dunsford, P. J. Rushworth, D. G. Hulcoop, R. A. Layfield, M. J. Ingleson, *Chem. Eur. J.* **2017**, *23*, 15889 – 15893; c) N. Miyaura, T. Ishiyama, M. Ishikawa, A. Suzuki, *Tetrahedron Lett.* **1986**, *27*, 6369 – 6372; d) H. Doucet, *Eur. J. Org. Chem.* **2008**, 2013 – 2030; e) C.-T. Yang, Z.-Q. Zhang, Y.-C. Liu, L. Liu, *Angew. Chem. Int. Ed.* **2011**, *50*, 3904 – 3907; *Angew. Chem.* **2011**, *123*, 3990 – 3993; f) A. Chatupheeraphat, H.-H. Liao, W. Srimontree, L. Guo, Y. Minenkov, A. Poater, L. Cavallo, M. Rueping, *J. Am. Chem. Soc.* **2018**, *140*, 3724 – 3735; g) G. A. Molander, C.-S. Yun, M. Ribagorda, B. Biolatto, *J. Org. Chem.* **2003**, *68*, 5534 – 5539.

[3] a) J. Choi, G. C. Fu, *Science* **2017**, *356*, eaaf7230; b) B. Saito, G. C. Fu, *J. Am. Chem. Soc.* **2007**, *129*, 9602 – 9603; c) M. S. Santos, A. G. Corrêa, M. W. Paixão, B. König, *Adv. Synth. Catal.* **2020**, *362*, 2367 – 2372; d) T. Hatakeyama, T. Hashimoto, K. K. A. D. S. Kathriarachchi, T. Zenmyo, H. Seike, M. Nakamura, *Angew. Chem. Int. Ed.* **2012**, *51*, 8834 – 8837; *Angew. Chem.* **2012**, *124*, 8964 – 8967; e) X. Lu, B. Xiao, L. Liu, Y. Fu, *Chem. Eur. J.* **2016**, *22*, 11161 – 11164; f) K. Komeyama, T. Michiyuki, I. Osaka, *ACS Catal.* **2019**, *9*, 9285 – 9291.

[4] a) N. Miyaura, K. Yamada, A. Suzuki, *Tetrahedron Lett.* **1979**, *20*, 3437 – 3440; b) G. A. Molander, B. W. Katona, F. Machrouhi, *J. Org. Chem.* **2002**, *67*, 8416 – 8423; c) T. Morishita, H. Yoshida, J. Ohshita, *Chem. Commun.* **2010**, *46*, 640 – 642; d) D. Alonso, C. Nájera, M. Pacheco, *Adv. Synth. Catal.* **2003**, *345*, 1146 – 1158; e) "Coupling Reactions Between C(sp^2) and C(sp) Carbon Centers": D. Gelman, I. Shaposhnikov in *Comprehensive Organic Synthesis II* (Ed.: P. Knochel), Elsevier, Amsterdam, **2014**, ch. 3.09, pp. 465 – 527; f) D.-L. Zhu, R. Xu, Q. Wu, H.-Y. Li, J.-P. Lang, H.-X. Li, *J. Org. Chem.* **2020**, *85*, 9201 – 9212.

[5] a) S. V. Damle, D. Seomoon, P. H. Lee, *J. Org. Chem.* **2003**, *68*, 7085 – 7087; b) G. Ebert, R. D. Rieke, *J. Org. Chem.* **1984**, *49*, 5280 – 5282; c) H. A. Stefani, A. S. Guarezemini, R. Cella, *Tetrahedron* **2010**, *66*, 7871 – 7918.

[6] a) N. Miyaura, K. Yamada, H. Suginome, A. Suzuki, *J. Am. Chem. Soc.* **1985**, *107*, 972 – 980; b) Y. Shi, X. Li, J. Liu, W. Jiang, L. Sun, *Tetrahedron Lett.* **2010**, *51*, 3626 – 3628; c) S. Thapa, B. Shrestha, S. K. Gurung, R. Giri, *Org. Biomol. Chem.* **2015**, *13*, 4816 – 4827.

[7] a) Y. Li, J. He, H. Shen, *Chem. Eur. J.* **2020**, *26*, 12310 – 12321; b) Y. Li, K. M.-C. Wong, H.-L. Wong, V. W.-W. Yam, *ACS Appl. Mater. Interfaces* **2016**, *8*, 17445 – 17453; c) W. E. Lindsell, P. N. Preston, J. M. Seddon, G. M. Rosair, T. A. J. Woodman, *Chem. Mater.* **2000**, *12*, 1572 – 1576; d) X. Gao, H. Liu, D. Wang, J. Zhang, *Chem. Soc. Rev.* **2019**, *48*, 908 – 936.

[8] a) P. Cadiot, W. Chodkiewicz in *Chemistry of Acetylenes* (Eds.: H. G. Viehe), Marcel Dekker, New York, **1969**, ch. 9; b) W. Shi, A. Lei, *Tetrahedron Lett.* **2014**, *55*, 2763 – 2772; c) P. Siemsen, R. C. Livingston, F. Diederich, *Angew. Chem. Int. Ed.* **2000**, *39*, 2632 – 2657; *Angew. Chem.* **2000**, *112*, 2740 – 2767; d) S. Verlinden, S. Ballet, G. Verniest, *Eur. J. Org. Chem.* **2016**, 5807 – 5812; e) V. Lavallo, G. Frey, B. Donnadieu, M. Soleilhavoup, G. Bertrand, *Angew. Chem. Int. Ed.* **2008**, *47*, 5224 – 5228; *Angew. Chem.* **2008**, *120*, 5302 – 5306.

[9] a) W. Heydenreuter, E. Kunold, S. A. Sieber, *Chem. Commun.* **2015**, *51*, 15784 – 15787; b) A. L. K. Shi Shun, R. R. Tykwinski, *Angew. Chem. Int. Ed.* **2006**, *45*, 1034 – 1057; *Angew. Chem.* **2006**, *118*, 1050 – 1073; c) X. Mo, A. Letort, D.-A. Roşca, K. Higashida, A. Fürstner, *Chem. Eur. J.* **2018**, *24*, 9667 – 9674; d) J. S. Lampkowski, D. M. Uthappa, J. F. Halonski, J. C. Maza, D. D. Young, *J. Org. Chem.* **2016**, *81*, 12520 – 12524; e) D. A. Barancelli, A. C. Mantovani, C. Jesse, C. W. Nogueira, G. Zeni, *J. Nat. Prod.* **2009**, *72*, 857 – 860.

[10] a) J. Berná, S. M. Goldup, A.-L. Lee, D. A. Leigh, M. D. Symes, G. Teobaldi, F. Zerbetto, *Angew. Chem. Int. Ed.* **2008**, *47*, 4392 – 4396; *Angew. Chem.* **2008**, *120*, 4464 – 4468; b) L. D. Movsisyan, M. Franz, F. Hampel, A. L. Thompson, R. R. Tykwinski, H. L. Anderson, *J. Am. Chem. Soc.* **2016**, *138*, 1366 – 1376; c) M. Franz, J. A. Januszewski, F. Hampel, R. R. Tykwinski, *Eur. J. Org. Chem.* **2019**, 3503 – 3512; d) J. D. Crowley, S. M. Goldup, N. D. Gowans, D. A. Leigh, V. E. Ronaldson, A. M. Z. Slawin, *J. Am. Chem. Soc.* **2010**, *132*, 6243 – 6248; e) Y. Sato, R. Yamasaki, S. Saito, *Angew. Chem. Int. Ed.* **2009**, *48*, 504 – 507; *Angew. Chem.* **2009**, *121*, 512 – 515.

[11] a) B. J. Eckstein, F. S. Melkonyan, N. Zhou, E. F. Manley, J. Smith, A. Timalsina, R. P. H. Chang, L. X. Chen, A. Facchetti, T. J. Marks, *Macromolecules* **2017**, *50*, 1430 – 1441; b) Y. Arakawa, S. Nakajima, S. Kang, M. Shigeta, G.-I. Konishi, J. Watanabe, *J. Mater. Chem.* **2012**, *22*, 13908 – 13910; c) B. Pigulski, N. Gulia, S. Szafert, *Eur. J. Org. Chem.* **2019**, 1420 – 1445.

[12] a) F. Diederich, P. J. Stang, R. R. Tykwinski, *Acetylene Chemistry: Chemistry, Biology and Material Science*, Wiley-VCH, Weinheim, **2005**; b) S. S. Eisler, A. D. Slepkov, E. Elliott, T. Luu, R. McDonald, F. A. Hegmann, R. Rik, R. R. Tykwinski, *J. Am. Chem. Soc.* **2005**, *127*, 2666 – 2676; c) M. Štefko, M. D. Tzirakis, B. Breiten, M.-O. Ebert, O. Dumele, W. B. Schweizer, J.-P. Gisselbrecht, C. Boudon, M. T. Beels, I. Biaggio, F. Diederich, *Chem. Eur. J.* **2013**, *19*, 12693 – 12704.

[13] a) W. Wu, H. Jiang, *Acc. Chem. Res.* **2014**, *47*, 2483 – 2504; b) P. C. Knutson, H. E. Fredericks, E. M. Ferreira, *Org. Lett.* **2018**, *20*, 6845 – 6849; c) Z. Chen, H. Jiang, A. Wang, S. Yang, *J. Org. Chem.* **2010**, *75*, 6700 – 6703; d) W. Shi, Y. Luo, X. Luo, L. Chao, H. Zhang, J. Wang, A. Lei, *J. Am. Chem. Soc.* **2008**, *130*, 14713 – 14720; e) S. Radhika, N. A. Harry, M. Neetha, G. Anilkumar, *Org. Biomol. Chem.* **2019**, *17*, 9081 – 9094.

[14] a) W. Li, J. K. Boon, Y. Zhao, *Chem. Sci.* **2018**, *9*, 600 – 607; b) S. Wang, M. Wang, L. Wang, B. Wang, P. Li, J. Yang, *Tetrahedron* **2011**, *67*, 4800 – 4806.

[15] S. Sarkar, P. Sarkar, P. Ghosh, *Org. Lett.* **2018**, *20*, 6725 – 6729.

[16] a) S. O. Kang, J. M. Llinares, V. W. Day, K. Bowman-James, *Chem. Soc. Rev.* **2010**, *39*, 3980 – 4003; b) M. Zhang, X. Yan, F. Huang, Z. Niu, H. W. Gibson, *Acc. Chem. Res.* **2014**, *47*, 1995 – 2005; c) K. Acharyya, P. S. Mukherjee, *Angew. Chem. Int. Ed.* **2019**, *58*, 8640 – 8653; *Angew. Chem.* **2019**, *131*, 8732 – 8745; d) A. Verma, K. Tomar, P. K. Bharadwaj, *Inorg. Chem.* **2019**, *58*, 1003 – 1006; e) A. K. Mandal, M. Suresh, P. Das, A. Das, *Chem. Eur. J.* **2012**, *18*, 3906 – 3917; f) S. Chakraborty, S. Saha, L. M. P. Lima, U. Warzok, S. Sarkar, B. Akhuli, M. Nandi, S. Bej, N. N. Adarsh, C. A. Schalley, R. Delgado, P. Ghosh, *J. Org. Chem.* **2017**, *82*, 10007 – 10014; g) L. K. S. von Krbek, C. A. Schalley, P. Thordarson, *Chem. Soc. Rev.* **2017**, *46*, 2622 – 2637; h) M. Gangopadhyay, A. K. Mandal, A. Maity, S. Ravindranathan, P. R. Rajamohanan, A. Das, *J. Org. Chem.* **2016**, *81*, 512 – 521; i) S. K. Samanta, M. Schmittel, *Org. Biomol. Chem.* **2013**, *11*, 3108 – 3115.

[17] a) C. Tan, D. Chu, X. Tang, Y. Liu, W. Xuan, Y. Cui, *Chem. Eur. J.* **2019**, *25*, 662 – 672; b) D. Zhang, A. Martinez, J.-P. Dutasta, *Chem. Rev.* **2017**, *117*, 4900 – 4942; c) A. Goswami, S. Gaikwad, M. Schmittel, *Chem. Eur. J.* **2021**, *27*, 2997 – 3001; d) S. S. Nurttila, W. Brenner, J. Mosquera, K. M. van Vliet, J. R. Nitschke, J. N. H. Reek, *Chem. Eur. J.* **2019**, *25*, 609 – 620; e) P. Sarkar, S. Sarkar, P. Ghosh, *Beilstein J. Org. Chem.* **2019**, *15*, 1505 – 1514; f) C. J. Brown, F. D. Toste, R. G. Bergman, K. N. Raymond, *Chem. Rev.* **2015**, *115*, 3012 – 3035; g) Z. Qi, C. Wu, P. Malo de Molina, H. Sun, A. Schulz, C. Griesinger, M. Gradzielski, R. Haag, M. B. Ansorge-Schumacher, C. A. Schalley, *Chem. Eur. J.* **2013**, *19*, 10150 – 10159.

[18] a) G. Anderegg, Z. Melichar, *Helv. Chim. Acta* **1993**, *76*, 1964 – 1969; b) S. N. Bhattacharya, C. V. Senoff, *Inorg. Chim. Acta* **1980**, *41*, 67 – 69; c) C. V. Senoff, *Inorg. Chem.* **1978**, *17*, 2320 – 2322.

[19] a) C. B. Aakeröy, M. Baldrighi, J. Desper, P. Metrangolo, G. Resnati, *Chem. Eur. J.* **2013**, *19*, 16240 – 16247; b) J. V. Alegre-Requena, A. Valero-Tena, I. G. Sonsona, S. Uriel, R. P. Herrera, *Org. Biomol. Chem.* **2020**, *18*, 1594 – 1601; c) O. Dumele, D. Wu, N. Trapp, N. Goroff, F. Diederich, *Org. Lett.* **2014**, *16*, 4722 – 4725; d) R. L. Sutar, S. M. Huber, *ACS Catal.* **2019**, *9*, 9622 – 9639; e) M. D. Perera, C. B. Aakeröy, *New. J. Chem.* **2019**, *43*, 8311 – 8314; f) J. Lieffrig, O. Jeannin, M. Fourmigué, *J. Am. Chem. Soc.* **2013**, *135*, 6200 – 6210; g) A. Matsuzawa, S. Takeuchi, K. Sugita, *Chem. Asian J.* **2016**, *11*, 2863.

[20] a) K. Miyamoto, Y. Yokota, T. Suefuji, K. Yamaguchi, T. Ozawa, M. Ochiai, *Chem. Eur. J.* **2014**, *20*, 5447 – 5453; b) M. Ochiai, K. Miyamoto, M. Shiro, T. Ozawa, K. Yamaguchi, *J. Am. Chem. Soc.* **2003**, *125*, 13006 – 13007; c) M. Ochiai, T. Suefuji, K. Miyamoto, M. Shiro, *Org. Lett.* **2005**, *7*, 2893 – 2896; d) V. Nemec, T. Piteša, T. Friščić, D. Cinčić, *Cryst. Growth Des.* **2020**, *20*, 3617 – 3624.

[21] M. Nilsson, *J. Magn. Reson.* **2009**, *200*, 296 – 302.

[22] D. L. Widner, E. R. Robinson, A. B. Perez, H. G. Vang, R. A. Thorson, Z. L. Driscoll, S. M. Giebel, C. W. Berndt, E. Bosch, E. D. Speetzen, N. P. Bowling, *Eur. J. Org. Chem.* **2017**, *2017*, 5739 – 5749.

[23] L. P. E. Yunker, R. L. Stoddard, J. S. McIndoe, *J. Mass Spectrom.* **2014**, *49*, 1 – 8.

[24] D. Lehnherr, J. M. Alzola, E. B. Lobkovsky, W. R. Dichtel, *Chem. Eur. J.* **2015**, *21*, 18122 – 18127.

[25] N. Iqbal, N. Iqbal, S. S. Han, E. J. Cho, *Org. Biomol. Chem.* **2019**, *17*, 1758 – 1762.

Manuscript received: December 18, 2020
Accepted manuscript online: January 13, 2021
Version of record online: March 18, 2021